Environmental Health Perspectives
Vol. 89, pp. 137-144, 1990

Experimental Lead Nitrate Poisoning: Microscopic and Ultrastructural Study of the Gills of Tench (*Tinca tinca, L.*)

by V. Roncero,* J. A. Vincente,* E. Redondo,* A. Gazquez,* and E. Duran*

A microscopic, ultrastructural, and morphometric study was made of the gills of tench (*Tinca tinca, L.*) subjected to acute experimental lead nitrate poisoning. Twenty-one adult tench were subjected to poisoning and a further 22 were used as controls. Lesions were characterized by the appearance of edema and epithelial hyperplasia and necrosis, both in cells forming part of the filtration barrier and in those in the interlamellar space. These processes developed in the course of the experiment, leading to the death of tench after 12 to 15 days of exposure to 75 ppm lead nitrate, at which point the concentrations of lead in the gills had reached their maximum.

Introduction

Lead, one of the highly toxic heavy metals, is being found in increasingly high amounts in living matter, in both marine and terrestrial ecosystems, largely due to the continuous and increasing pollution of the environment by industrialized regions all over the world.

The abundant sources of environmental pollution involving lead include fumes from combustion engines, the dumping of industrial waste, the use of lead piping for water supplies, and the use in the past of lead-based paints. This pollution gives rise to the progressive accumulation of lead compounds in the aquatic environment (*1-8*).

The gills by which teleosts oxygenate their blood are highly suitable in their orientation and morphology, a large surface area being exposed to a constant flow of water that moves in the opposite direction to the flow of blood in that area. The secondary lamellae are in constant and direct contact with the water and are thus highly sensitive to any change in water condition or composition (*9*). Such changes directly affect gill structure (*10*) and ultimately affect the whole organism. Fish are therefore the most appropriate species to act as biological indicators of water pollution levels.

Although many studies have been made of lead poisoning in mammals, most deal with chronic processes, from exposure to and progressive accumulation of small quantities of lead until toxic levels are finally reached. As a heavy metal, lead has a particular affinity for gastrointestinal absorption in both mammals (*11,12*) and teleosts (*13,14*). In mammals (*15*), 60% of lead accumulates in bone tissue, 25% in liver tissue, and 4 to 5% in renal parenchyme, although in acute processes the highest levels are found in the liver and the kidney.

The purpose of this study was to identify the acute lesions caused by experimental lead nitrate poisoning in fish gills, specifically about structures forming part of the respiratory barrier, and to consider the possible extrapolation of the results to other animals in future investigations.

Materials and Methods

The 43 adult tench (*Tinca tinca L.*) used in this experiment were sacrificed as shown in Table 1. The experiment was carried out in a 250-L tank, where tench were kept for 24 hr without eating in order to acclimate to the water quality, oxygenation, and a temperature of 17 to 20°C. The lead nitrate dosage used was 75 mg/L of water. The tench, which were supplied by the Centro Nacional de Ciprinicultura Vegas del Guadiana, Badajoz, Spain, were of an average length of 25 to 30 cm and weighed roughly 200 g; gender was not taken into account.

Table 1. Batch distribution.

Batch	Number of tench	Duration of exposure
I	3	24 hr
II	3	48 hr
III	3	4 days
IV	3	7 days
V	3	9 days
VI	3	12 days
VII	3	15 days
Control	22	(Same duration as experiment)
Total	43	

*Department of Histology and Pathological Anatomy, Faculty of Veterinary Sciences, Caceres, Spain.

Address reprint requests to V. Roncero, Department Histologia y Anatomia Patologica, Facultad de Veterinaria, 10071-Caceres, Espana.

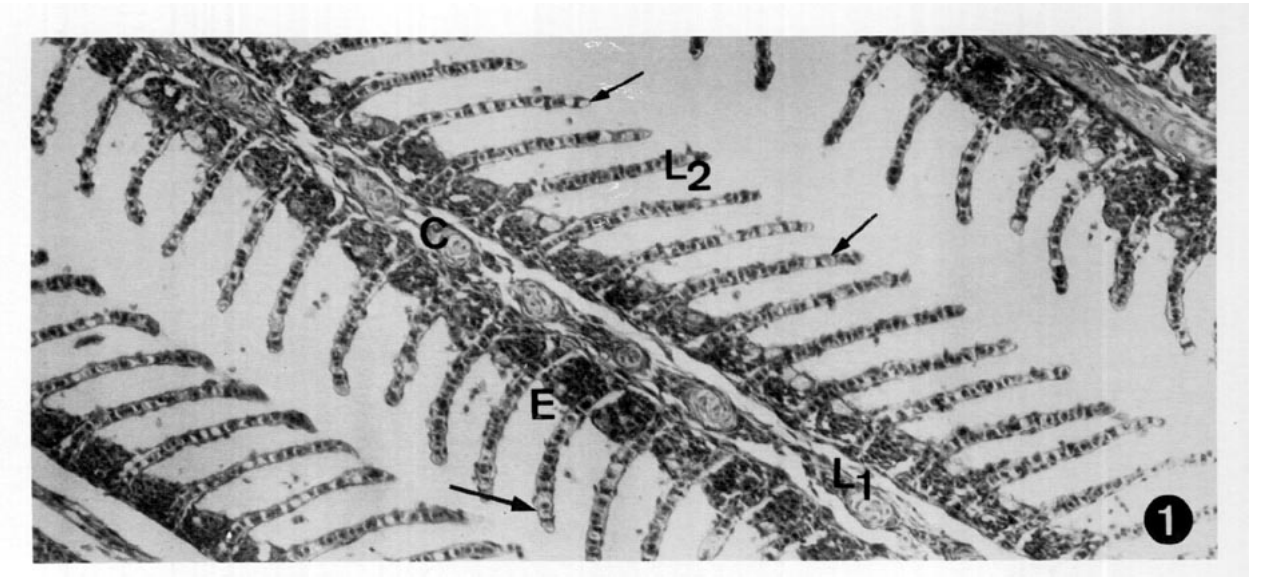

FIGURE 1. Control group. Primary lamellae of tench gill arches (L_1) with a central hyaline cartilage (C). Secondary lamellae (L_2) perpendicular to the primary lamellae, with abundant vascular spaces (arrows) and a multi-layered interlamellar epithelium (E).

Immediately after decapitation, the gills were extracted and fixed in 5% glutaraldehyde for light and electron microscopy. Samples for structural study were processed according to routine light microscopy techniques and embedded in paraffin. Sections were stained with hematoxylin-eosin and PAS. Samples for ultrastructural study were prepared according to the methods outlined by Sabatini et al. (*16*) and were embedded in Durcapan (ACM).

Samples for scanning electron microscopy were fixed in 5% phosphate-buffered glutaraldehyde, placed in an aqueous solution containing 2% glycine, 2% saccharose, and 2% tannic sodium glutamate, and postfixed in 2% osmium tetroxide prior to dehydration in a graded series of acetones.

The level of lead in gills was determined in all tench from each batch by means of a quantitative analysis using atomic absorption spectrophotometry (Perkin-Elmer 380). A Vids-III semiautomatic image analyzer was used for morphometric analysis, and over 100 secondary lamellae per fish from all the different batches from were measured.

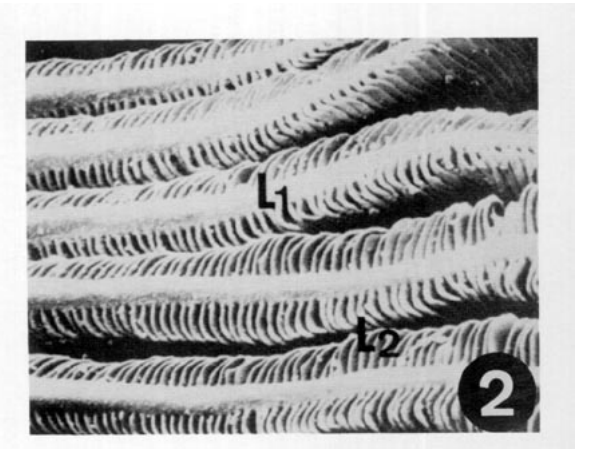

FIGURE 2. Control batch. Primary (L_1) and secondary (L_2) branchial filaments seen through scanning electron microscope.

Results

Tench gill arches are composed of numerous primary lamellae (Figs. 1 and 2), which have a cartilaginous central structure and are highly vascularized. Two rows of secondary lamellae run perpendicular to each primary lamella (Figs. 1 and 2), flattened and delimited by a simple flat, fine epithelium. These secondary lamellae, together with the central vascular spaces, form the gaseous exchange barrier, or respiratory barrier. The structure is supported by pillar cells.

The interlamellar space contains a multilayered epithelium composed of numerous cells and supported by a visible basal membrane that separates the cells from the vascular and cartilaginous structures of the primary and secondary

Table 2. Morphometric analysis of the secondary lamellae of tench gills after exposure to lead nitrate.[a]

Batch	Average area, μm	SE (internal)	SE (Pooled)	99% Confidence intervals for mean
Control	1333.9	25.985	17.764	1288.03-1379.79
I	802.5	21.592	21.303	747.51- 857.44
II	557.5	11.722	18.449	509.89- 605.18
III	720.7	25.556	25.375	655.20- 786.27
IV	625.0	14.971	19.927	573.59- 676.52
V	626.7	19.128	21.939	570.09- 683.41
VI	962.1	31.431	30.566	883.19-1041.07
VII	826.8	23.707	29.984	749.41- 904.28
Mean	815.9	7.751	7.751	795.90- 835.94

[a] $p < 0.001$ (99.99%) for all batches.

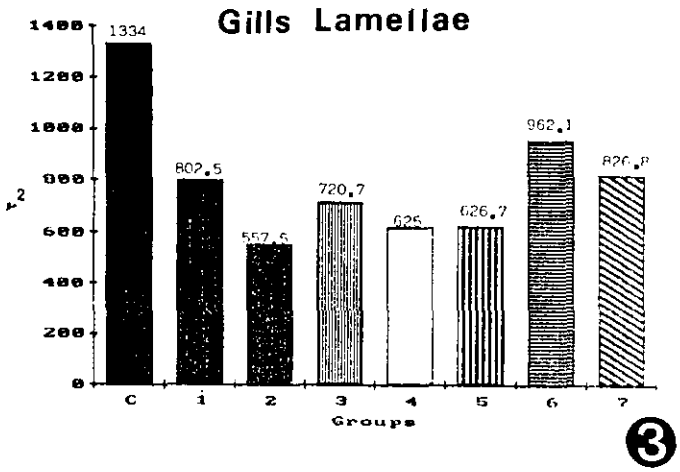

FIGURE 3. Tench gill lamellae, from the control batch and different experimental batches.

Table 3. Lead concentration in gills.

Group	Batch	Exposure duration	Fresh weight
	Control	—	3.8 mg/kg
1	I	24 hr	30.6 mg/kg
	II	48 hr	33.2 mg/kg
2	III	4 days	46.5 mg/kg
	IV	7 days	53.2 mg/kg
3	V	9 days	140 mg/kg
4	VI	12 days	120 mg/kg
	VII	15 days	200 mg/kg

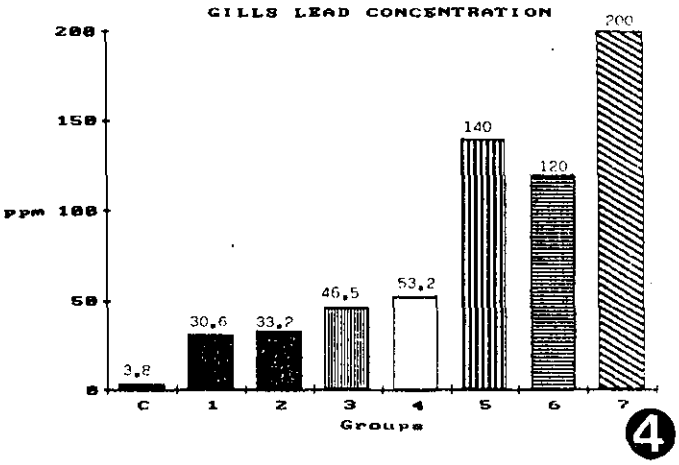

FIGURE 4. Gill lead concentration in control batch and various experimental batches, showing an increase in lead concentrations as the experiment progresses.

filaments. The cell types involved are epithelial cells, chloride cells, mucous, and granular cells; the basal border contains a large number of as yet undifferentiated cells.

Prior to discussing the lesions, we have included the measurements of several parameters for the secondary lamellae of gills of both experimental and control fish from all batches. These values are shown in Table 2 and Figure 3. Similarly, measurements were made of the amount of lead

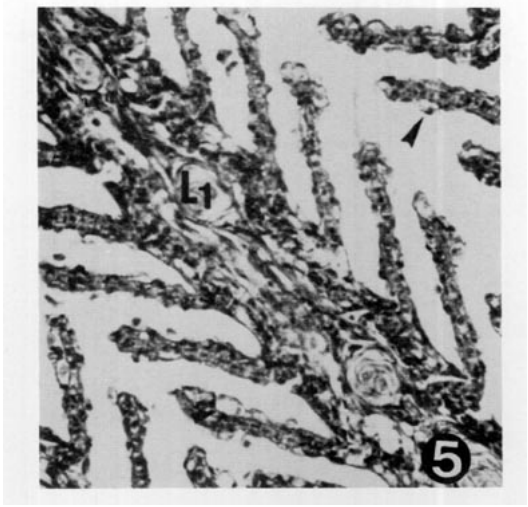

FIGURE 5. Batch I. Gill lamina (L_1), with numerous secondary lamellae (L_2). Marked edema (arrow) in the respiratory epithelium.

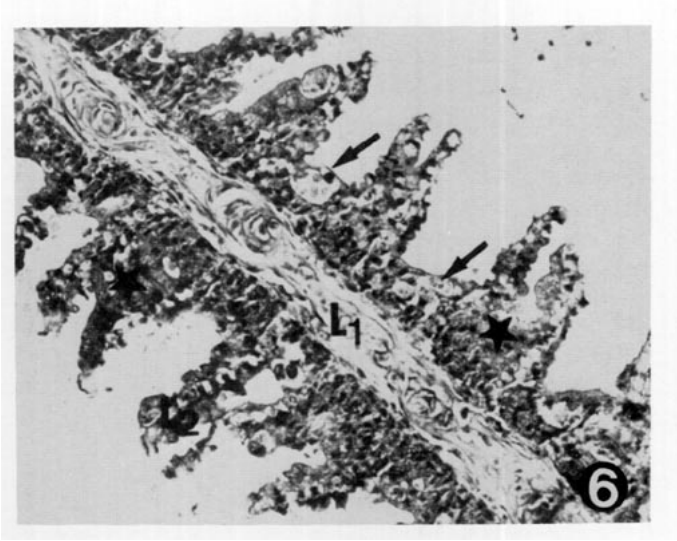

FIGURE 6. Batch IV. Gill lamella (L_1) showing considerable epithelial hyperplasia (★) in the secondary lamella (L_1) and the interlamellar space, where small areas of focal necrosis are visible (arrows).

(mg/kg or ppm) accumulated in the gill parenchyma both for control and experimental batches. The results are shown in Table 3 and Figure 4.

Histopathological lesions observed were common to the different batches and continued to develop until the end of the experiment. To facilitate description, the batches have been classified into four groups (Table 3).

Group 1

Group 1 included batches I and II, sacrificed 24 and 48 hr respectively, after the start of the experiment. Light microscopy revealed a decrease in the surface area of the secondary lamella (Fig. 3) from 1333.9 μm in the control batch to 557.5 μm in batch II (Table 2).

Structurally, lesions tended to appear in the secondary lamellae, where an edema of the respiratory epithelium was observed in the medio-distal region of the lamellae (Figs. 5 and 6). This process did not occur in adjacent vascular lumina. No lesions were observed in the epithelium of the interlamellar space.

Electron microscope analysis of the respiratory epithelium confirmed the existence of a severe intercellular edema of the respiratory barrier, affecting both superficial and basal epithelial cells. In this area, focal retractions were observed of the basal membrane which separates it from the vascular epithelium (Fig. 7).

The cytoplasm of respiratory epithelial cells, though not particularly electron dense, contained highly developed lysosomes. Small cytoplasmic protrusions, in the form of microvilli, were found in the free apical border. In the earlier batches, these protrusions were generally coated with abundant, fine, highly electron-dense granular material (Fig. 7). Accumulated lead concentration in gills during the first 2 days of the experiment reached 33.2 mg/kg (Table 3).

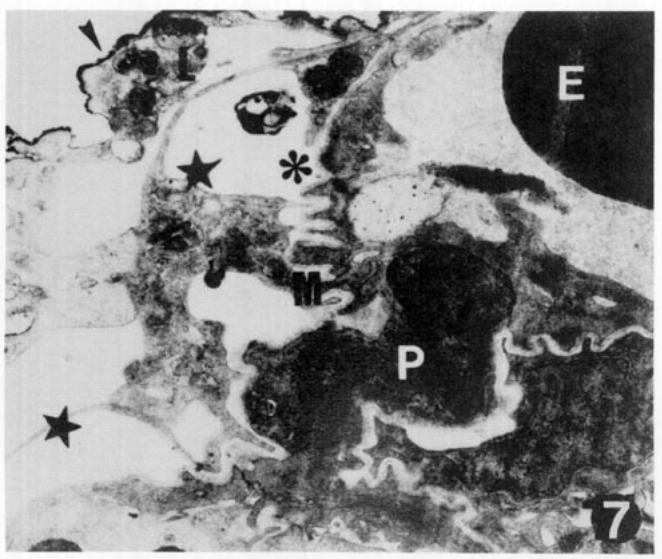

FIGURE 7. Batch I. Secondary lamella ultrastructure. Erythrocyte (E), pillar cell (P). Edema in the respiratory epithelium (★). Lead particles adhering to the cell surface (arrows). Disorganization of the basal membrane of the respiratory barrier (★).

Group 2

Group 2 was composed of batches III and IV, sacrificed 4 and 7 days, respectively, after the start of the experiment. Though the average surface area of secondary lamellae in these batches was smaller than that of controls (Fig. 3), it had risen slightly with respect to batch II.

Light microscopic analysis showed a continuation of the edema in the secondary lamellae, and the beginning of a marked epithelial proliferation both in the lamellae and within the interlamellar space itself (Fig. 6), where small areas of necrosis had begun to appear.

Ultrastructural examination confirmed the lamellar edema already observed in group 1, together with the disorganization of the basal membrane. Small areas of necrosis were observed in the cytoplasm of respiratory epithelial cells (Fig. 8), and interlamellar epithelial chloride cells (Fig. 9). Necrotic areas contained electron-dense granular material of undefined morphology.

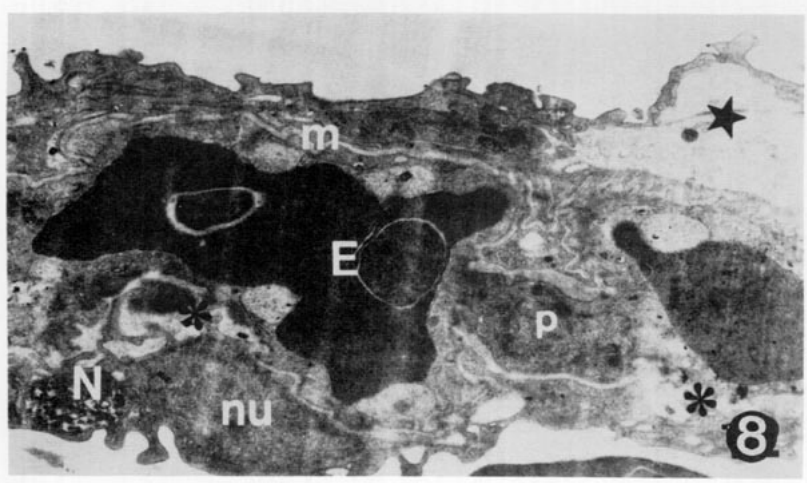

FIGURE 8. Batch III. Secondary lamella showing evident edema (★) and necrosis of the respiratory epithelium (N). Disorganization (★) of the basal membrane (m) of the respiratory barrier; erythrocyte (E). Pillar cell (P).

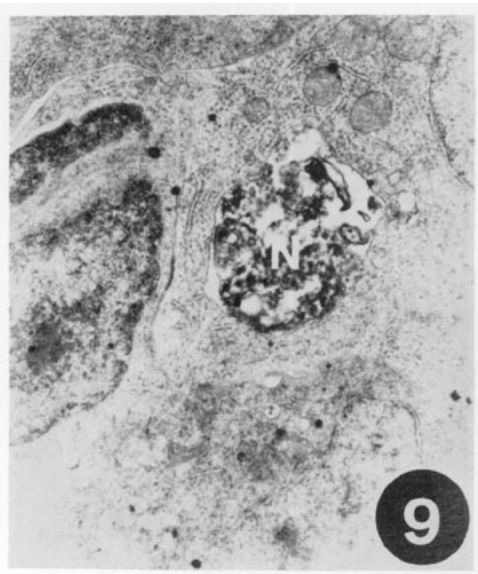

FIGURE 9. Batch IV. Marked focal necrosis (N) of chloride cells in the interlamellar space.

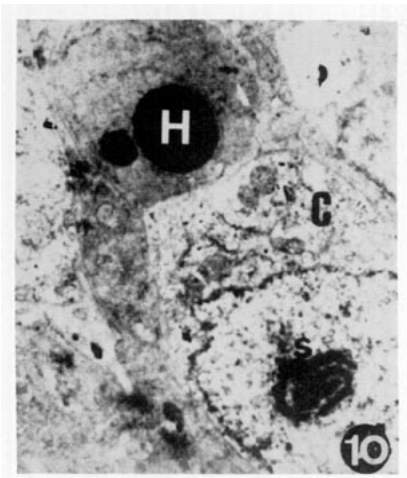

FIGURE 10. Batch III. Spherical, highly electron-dense vacuoles (H), with nucleolar segregation (S) of a chloride cell (C).

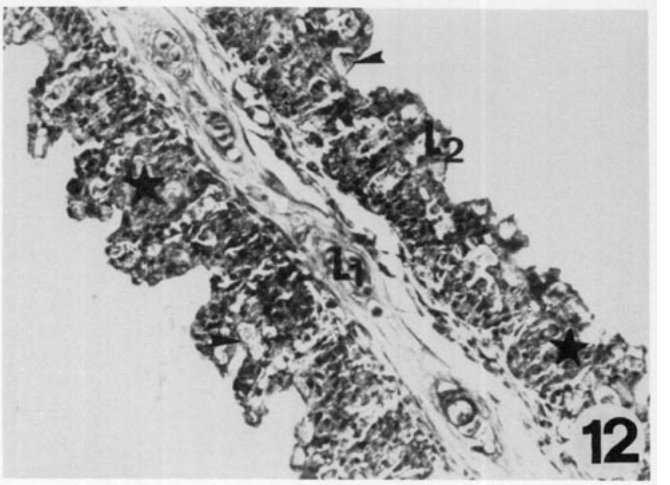

FIGURE 12. Batch VII. Primary branchial filament (L_1) showing marked epithelial proliferation (★) completely covering the secondary lamella (L_2). Numerous necrotic foci (arrows) throughout the filament.

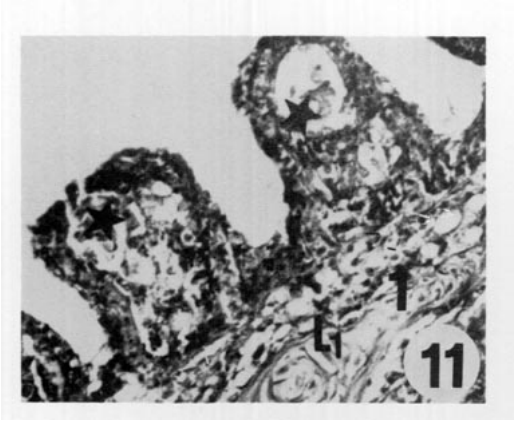

FIGURE 11. Batch VI. Fusion and total necrosis of secondary lamellae (★).

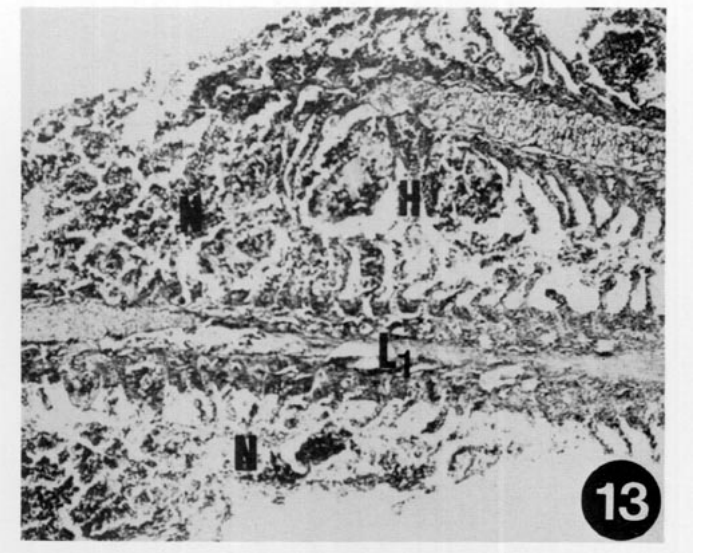

FIGURE 13. Batch VII. Branchial filaments (L_1) showing severe and extensive necrosis (N) and consequent cellular desquamation.

Interlamellar epithelial cells also contained highly electron-dense spherical vacuoles occupying part of the cytoplasm. Chloride cell nuceli contained scant euchromatin, and nucleolar segregation was observed (Fig. 10). The concentration of accumulated lead in gills after 7 days had risen progressively to 53.2 mg/kg (Table 3).

Group 3

Group 3 consisted of tench from batch V, sacrificed 9 days after the start of the experiment. The mean surface area of the secondary lamellae in this group was similar to that of group 2 (Table 2), but the concentration of accumulated lead after 9 days had reached 140 mg/kg (Table 3). Lesions observed were broadly similar to those of group 2, though areas of necrosis had obviously grown.

Group 4

Group 4 was formed by batches VI and VII, sacrificed at 12 and 15 days, respectively, after the start of the experiment. Although the mean surface area of secondary lamellae was smaller than controls, it was somewhat larger than in previous batches, reaching 826.8 μm in the last batch. Lesions at this stage, however, were so severe that they proved fatal to one tench from each of these batches.

Structural examination revealed fusion and partial necrosis of secondary lamellae (Fig. 11) and maximum proliferation of epithelial cells both in secondary lamellae and in the interlamellar space, totally covering the respiratory barrier (Fig. 12). Maximum necrosis was also reached in these batches (Fig. 13).

Scanning electron microscope analysis confirmed the

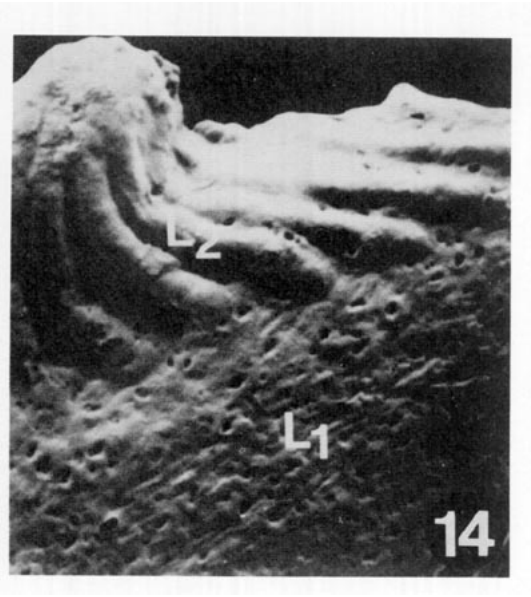

FIGURE 14. Batch VI. Fusion and partial necrosis of secondary lamellae. Scanning electron microscope.

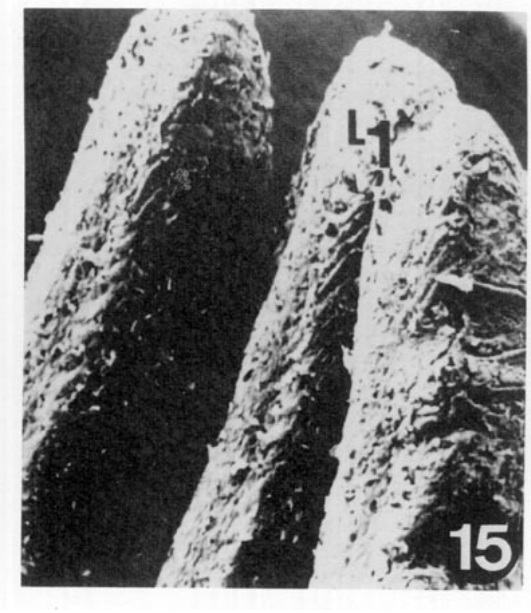

FIGURE 15. Batch VII. Primary branchial filaments (L_1); secondary lamellae have completely disappeared. Scanning electron microscope.

fusion of secondary lamellae (Fig. 14) and the subsequent disappearance of the secondary branchial filament (Fig. 15). Ultrastructural examination showed epithelial proliferation and severe necrosis (Fig. 16) in both epithelial and chloride cells at apical and basal positions in the interlamellar space. Mucous cells were apparently not affected, although abundant, electron-dense granular material was observed in muscle cells adjacent to the interlamellar space (Fig. 16).

The endothelium of blood capillaries contained numerous cytopemsis vesicles and fine, electron-dense granular material (Fig. 17) spreading as far as the erythrocytes of the capillary lumen, and in some cases forming considerable intracytoplasmic aggregates (Fig. 18).

In the final stages of the experiment, a marked uniform heterophil infiltration of the interlamellar space was observed (Fig. 19). The cytoplasm of these cells contained characteristic ellipsoid granulations and fine, electron-dense granular material scattered throughout the cell. The accumulated concentration of lead in the gills of tench sacrificed 15 days after the start of the experiment rose progressively to 200 mg/kg, although in batch VI a slight fall took place with regard to the previous batch (Table 3).

Discussion

Gill lesions in tench subjected to experimental lead nitrate poisoning are characterized primarily by marked hyperplasia of epithelial cells in the secondary lamella and the interlamellar space and by severe necrosis in both structure.

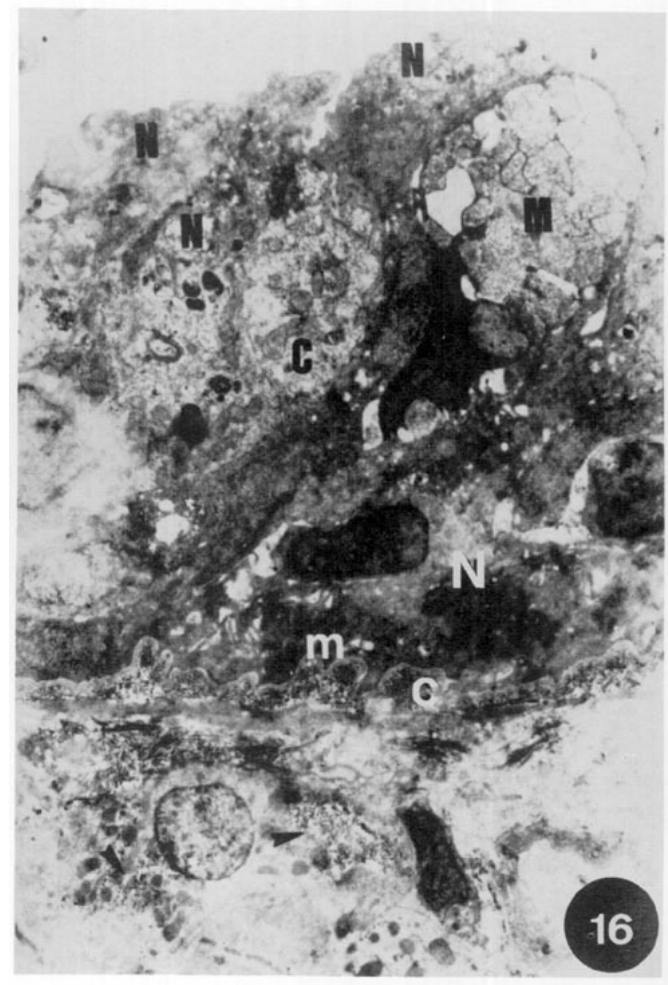

FIGURE 16. Batch VI. Interlamellar space. Severe necrosis (N) of epithelial cells and chloride cells (C) and less differentiated basal cells. Basal membrane (m); collagen fibers (c). Accumulation of lead particles in a fine granulate layer (arrowheads) in the cytoplasm of a muscle cell.

Although intranuclear or intracytoplasmic inclusions have been reported in kidney and liver of both mammals and fish subjected to acute lead poisoning (*11,12,17–20*), no such findings were made in tench gills. Electron microscopy, however, revealed abundant, fine, electron-dense granular material (*21*), which may constitute the initial stages of formation of inclusions.

The primary lesion in secondary lamellae was a severe edema detectable from the start of the experiment. The edema was located principally in the distal third of the lamella,

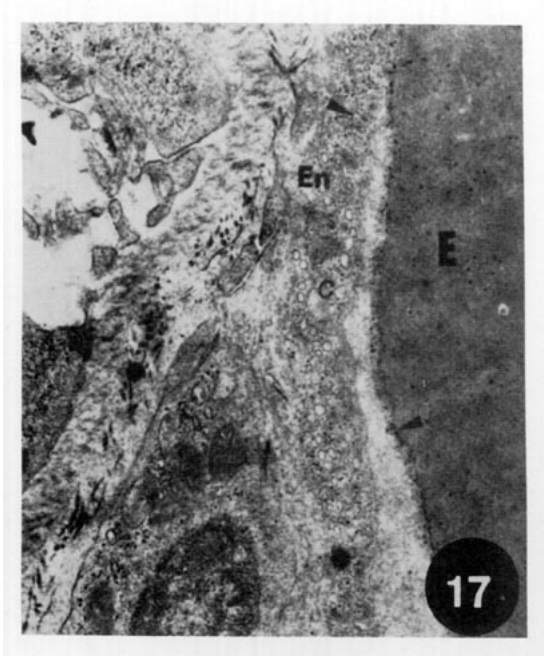

FIGURE 17. Batch VI. Gill capillary. Erythrocyte (E), vascular endothelium (En) with numerous cytopemsis vacuoles (c) and fine lead particles in the endothelium and the capillary lumen (arrowheads).

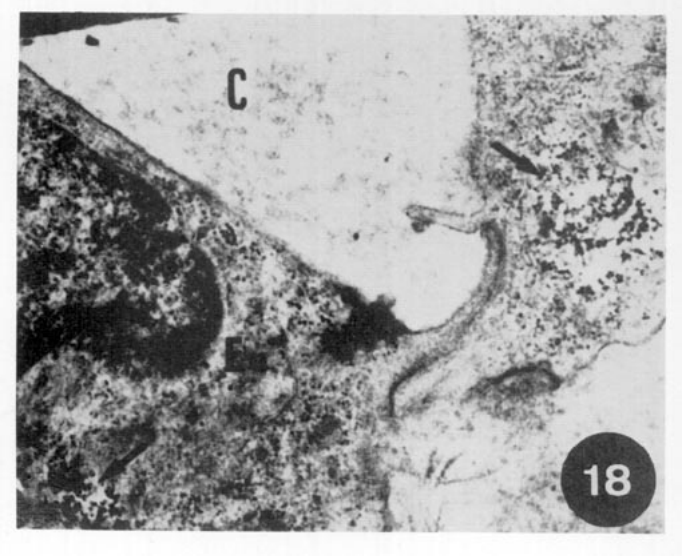

FIGURE 18. Batch VII. Endothelium (En) of capillary lumen (C), showing numerous lead particles forming clusters (arrows).

FIGURE 19. Batch VII. Interlamellar space, showing cell necrosis (N) and heterophilic infiltration (H). Numerous fine lead particles throughout the cytoplasm (arrowheads).

although other authors (*22*) report a clearly basal location.

Epithelial hyperplasia was noted as length of time exposed to lead increased in the experiment, accompanied by increasingly severe cell necrosis, evident from the start in the number of lysosomes, auto-phagosomes, and hetero-phagosomes. This may be attributed to the direct action of lead on cell membranes, giving rise to increased fragility (*15*). Massive mucous hyperproduction (*23*) was not observed at any stage of this experiment.

Lesions observed in secondary lamellae of the gills at all stages of the experiment resembled those reported by other authors (*22–24*) in similar processes, although in this experiment the location of lesions was not always the same.

Edema, epithelial hyperplasia, and necrosis gave rise to acute respiratory distress. This, coupled with the reduction in surface area of the respiratory barrier of the secondary lamellae, observed throughout the experiment, and the inhibition of enzyme mitochondrial transport systems (*24,25*), led to the inevitable death of the fish.

Fine, electron-dense granular material observed in the extracellular space and adhering to the respiratory barrier in the earliest batches spread to the cytoplasm of various cell types in the course of the experiment. References to this material have not ben found in the literature consulted,

although similar structures have been reported in nephron tubular epithelium in an identical experiment (*21*). It is felt that these structures are lead particles because of their capacity to form precipitates with carboxyl-rich protein (*20*).

As in similar processes, the multilayered epithelium of the interlamellar space was also affected (*20,22,24,25*). Necrosis was observed over the latter half of the experiment, becoming severe in the last batch. Epithelial and chloride cells were the worst affected; cytoplasmic organelles were in disarray, and a large number of lysosomes and electron-dense vacuoles (*21*) were evident. These structures specifically store large amounts of heavy metals such as mercury and zinc (*11*), although in this case they are felt to be a clear indication of cell degeneration.

No appreciable differences were noted in cell electron density (*24,25*), which was more a function of the degree to which cells were affected. Lead causes cell hyperactivity, with the resulting proliferation of chloride cells and a substantial increase in ion exchange (*25*), leading subsequently to degeneration and necrosis of cell elements, and a severe alteration in the osmotic regulation of the internal medium. These cells, together with nephron tubular epithelial cells, are responsible for maintaining the base-acid balance in the internal medium.

Toward the end of the experiment, the interlamellar epithelium was infiltrated by heterophilic blood cells (*23*). Cytoplasm contained fine, electron-dense granular material, similar to that observed in other areas, which is considered to be a direct cause of cell necrosis (*21*). It is felt that the presence of this granular material may be due to the phagocytic capacity of these cells, which appear when the lead concentration is at its highest point (Fig. 9).

In conclusion, it may be stated that tench gill lesions caused by experimental lead poisoning include hyperplasia and necrosis of epithelial cells in both the respiratory barrier and the interlamellar space. Those processes appeared 24 to 48 hr after administration of the lead nitrate, and at 9 days were completely developed, causing the death of tench in the last batches. The progressive severity of lesions to the gill was a function of lead concentration in different batches, lesions becoming more severe as accumulation increased (*26*), though not proportionately so.

Like other heavy metals, lead is manifestly accumulative and cannot be excreted. Therefore, the consumption of species that have already accumulated quantities of lead into their structures leads to higher rates of lead pollution, which continue to rise further up the food chain, reaching their maxima in predators.

REFERENCES

1. Boutron, C. Le plomb dans l'atomspher. La Recherche 81: 592–602 (1988).
2. Hernandez, L. M. Rico, M. C. Gonzalez, M. J., and Hernan, M. A. Environmental contamination by lead and cadmium in plants from urban area of Madrid, Spain. Bull. Environ. Contam. Toxicol. 38: 203–208 (1987).
3. Hutton, M., and Symon, C. The quantities of cadmium, lead, mercury and arsenic entering the U.K. environment from human activities. Total Environ. 57: 129–150.
4. Pascual, C, Quintana, R., Mayan, J. M., and Capont, L. Contribucion ecotoxicologica del cadmio y del plomo en el mejillon cultivado en Galicia. Alimentaria 175: 45–51 (1986).
5. Coello, W. F. Saleem, Z. A., and Khan, M. A. Q. Ecological effects of lead in auto-exhaust. In: Survival in Toxic Environments (M. A. Q. Khan and J. P. Bederka, Eds.,), Academic Press, Inc., New York, 1974, pp. 499–515.
6. Hurst, W. Medicina Interna. Panamericana, Buenos Aires, 1984.
7. Leonzio, C., Fossi, C., and Focardi, S. Lead, mercury, cadmium and selenium in two species of gull feeding on inland dumps and marine areas. Sci. Total Environ. 57: 121–127 (1986).
8. Starodub, M. E., Wong, P. T. S., Mayfield, C. I., and Chau, Y. K. Influence of complexation of pH on individual and combined heavy metals toxicity to a freshwater green alga. Can. J. Fish. Aquat. Sci. 44(6): 1173–1180 (1987).
9. Roncero, V., Redondo, E. Gazquez, A., and Duran, E. Structural and ultrastructural differntiation of cell types in the gills of the tench, Tinca tinca L. J. Vet. Med. C, in press.
10. Wong, M. H., Lau, W. M., Tong, T. Y., Liu, W. K., and Lunk, K. C. Toxic effects of chromic sulphate on the common carp (*Cyprinus carpio*). Toxicol. Lett. 10: 225–232 (1982).
11. Jones, T. C., and Hunt, R. D. Veterinary Pathology. Lea and Fabiger, Philadelphia, 1983.
12. Venugopal, S., and Luckey, T. D. Metal Toxicity in Mammals, Vol. 2. Chemical Toxicity of Metals and Metalloids. Plenum Press, New York, 1978, pp. 185–196.
13. Pequinot, J., and Moya, A. Effects of different toxins (Pb, Cu, Formol and NH4) on the carp: histologic changes in excretory and haematopoietic organs. Eur. J. Toxicol. Environ. Hyg. B: 361–369 (1975).
14. Pequinot, J., and Gire, M. P. Toxicity of lead nitrate to the carp (*Cyprinus carpio*). Effects on respiratory metabolism and histological structure of gill lamellas. Toxicol. Eur. Res. 1: 89–92, (1978).
15. Quer-Brossa, S. Toxicologia Industrial. Edt. Salvat S. A. Barcelona (1983).
16. Sabatini, D. D., Bensch, K., and Barnett, R. J. Cytochemistry and electron microscopy. The preservation of cellular structures and enzymatic activity by aldheyde fixation. J. Cell. Biol. 17: 19–58 (1963).
17. Reichenbach-Klinke, H. H. Enfermedades de los Peces. Edt. Acribia, Zaragoza (1982).
18. Forland, M., and Spargo, B. H. Clinicopathological Correlations in chronic Toxic Nephropathies. In: Laboratory Diagnosis of Diseases Caused by Toxic Agents (F. W. Sunderman, Ed.) Adam Hilger, London, 1970, pp. 436–450.
19. Gisbert, J. A. Medicina Legal y Toxicologia. Fundacion Garcia Muñoz. Sección Saber, Valencia (1983).
20. Fowler, B. A. Intracellular compartmentation of metals in aquatic organisms: roles in mechanisms of cell injury. Environ. Health Perspect. 71: 121–128 (1987).
21. Roncero, V., Gazquez, A., Redondo, E., Moyano, M. C., and Durán, E. Etude structurale et ultrastructurale du rein de la tanche, *Tinca tinca, L.* apres intoxication experimentale par absortion de nitrate de plomb. J. Vet. Med. A. 35: 529–543 (1988).
22. Roberts, R. J. Patologia de los Peces, Ed. Mundi-Prensa, Madrid (1982).
23. Krishnaja, A. P., Rege, M. S., and Joshi, A. B. Toxic effects of certain heavy metals (Hg, Cd, Pb, As and Se) on the intertidad crab, *Scylla serrata*. Mar. Environ. Res. 21: 109–119 (1987).
24. Rojik, I., Memcsok, J., and Boross, L. Morphological and biochemical studies on liver, kidney and gill of fishes affected by pesticides. Acta Biol. Hung. 34(1): 81–92 (1983).
25. Crespo. S., and Sala, R. Ultrastructural alterations of the dogfish (*Scyliorhinus cancicula*) gill filament related to experimental aquatic zinc pollution. Dis. Aquat. Org. 1: 99–104 (1986).
26. Villarreal-Treviño, C. M., and Villegas-Navarro, A. Differential accumulation of lead by soft tissues of rabbit. Bull. Environ. Contam. Toxicol. 39: 334–342 (1987).